Adaptive Equalization and Diversity Combining for Mobile Radio using Interpolated Channel Estimates

Norm W. K. Lo, *Student Member, IEEE,* David D. Falconer, *Fellow, IEEE,* and Asrar U. H. Sheikh, *Senior Member, IEEE*

Abstract—**Digital cellular radio (DCR) communications occur over a fading multipath channel. In the case of low bit-rate, narrow-band communications, some form of adaptive equalization and diversity combining is required to mitigate the intersymbol interference and rapid time variations in the DCR channel. In this paper, we demonstrate the feasibility of a DCR system which employs a jointly adaptive decision-feedback equalizer and diversity combiner. In particular, we utilize the current estimates of the channel impulse response (CIR) at each diversity branch to compute the receiver parameters periodically. Moreover, we propose a novel block-adaptive strategy which computes the time-varying CIR by interpolating a set of CIR estimates obtained through periodic training. Despite incurring some inherent processing delay and throughput reduction, this interpolation strategy has the advantage of immunity to decision errors which would quite likely occur during a deep fade. Furthermore, we discovered that the system performance is limited, in the form of an irreducible bit error rate at high signal-to-noise ratios (SNR), by the CIR estimation of the rapidly fading channel.**

Introduction

THE currently proposed North American standard for digital cellular radio (DCR) communications incorporates a narrow-band time division multiple access (TDMA) format with three users sharing a frequency channel of 30 kHz bandwidth. The overall bit rate is 48.6 kb/s, with each user data rate being about 13 kb/s. The modulation scheme is $\pi/4$-shifted differentially encoded quadrature phase shift keying (DQPSK).[1] Furthermore, to limit the adverse effects of adjacent channel interference (ACI), the proposed transmit and receive filters have small excess bandwidths corresponding to tight rolloffs of 35% [1].

However, with such stringent filtering, data dispersion spans several symbol periods and significantly increases the intersymbol interference (ISI) caused by multipath propagation. In addition, when mobiles are at highway speeds, the DCR channel exhibits Doppler fading rates of up to about 100 Hz. Consequently, for the relatively low symbol rate of 24.3 ks/s, a signal experiences rapid time variations. Given the worst-case scenario of severe ISI and fast fading, some form of adaptive equalization and diversity combining is required to overcome these channel impairments.

In this paper, we investigate the performance of a DCR reception technique employing adaptive equalization and diversity combining to mitigate the channel impairments of frequency-selectivity, Doppler fading and additive noise. The reduction of ISI is accomplished with a fractionally spaced decision-feedback equalizer, while the detrimental effect of fast fading is alleviated by block adaptation, explicit diversity combining and the implicit diversity which is inherent in a frequency-selective fading channel [2]. We do not investigate the effects of ACI; however, the tight filtering and diversity combining employed in the receiver would tend to minimize these interference effects.

We address the issue of the rapidly time-varying DCR channel by employing block adaptation based on a signaling format consisting of contiguous frames of transmitted data within a long TDMA time slot. Specifically, the start of each data frame contains a known training sequence which is used to estimate the impulse response of each diversity channel. However, the random time variation of a DCR channel can be quite severe during a typical data block sequence. Consequently, learning the channel at just the start of each data sequence is not sufficient to follow the time variations of the channel. Therefore, one must either increase the frequency of training (at the expense of a reduction in the system throughput) and/or track the fast fading channel with an adaptive algorithm.

As an example of the latter strategy, a continuous, symbol-by-symbol adaptive algorithm such as the least-mean-square (LMS) algorithm may be used to track the randomly changing CIR during a data block sequence. However, we have found that, due to its sensitivity to error propagation, the decision-directed LMS adaptive algorithm has difficulty tracking a 100 Hz Doppler DCR channel. A more complex adaptive algorithm such as the recursive least squares (RLS) algorithm would not improve the CIR tracking since it has been shown that LMS can perform CIR tracking at least as well as RLS [3], [4]. Furthermore, the RLS algorithm also suffers from error propagation in the decision-directed mode.

In this paper, we propose a novel method of block adaptation for tracking a time-varying CIR during a data sequence. Instead of explicitly tracking the time-varying CIR by using a continuous, decision-directed adaptive algorithm like LMS, we employ a block-adaptive strategy which computes the

Manuscript received October 5, 1990; revised December 10, 1990. This work was supported by Bell Northern Research (BNR) and by the Natural Sciences and Engineering Research Council (NSERC) of Canada.

The authors are with the Department of Systems and Computer Engineering, Carleton University, Ottawa, ON, Canada K1S 5B6.

IEEE Log Number 9100982.

[1] In $\pi/4$-shifted DQPSK, the conventional DQPSK signal is modified by inserting an additional 45°-phase rotation in every symbol interval.

0018-9545/91$01.00

time-varying CIR by interpolating a set of estimated CIR values obtained through periodic training at adjacent data frames within a given TDMA time slot. By using the interpolated CIR estimates, we periodically compute the receiver parameters to adapt it to the fast fading channel. While this adaptive strategy has the inherent disadvantages of processing delay and reduction in system throughput, it does have the key advantage of immunity to decision errors which can quite likely occur during a deep fade. In addition, this approach of computing the equalizer/combiner parameters with channel estimates differs from previously investigated, block adaptive schemes where the equalizer parameters are adapted directly [5].

While we consider the use of periodically inserted overhead bits for channel estimation and tracking, a DCR modem would likely use additional overhead bits in each frame as parity check bits for error correction. Such a block or convolutional coding scheme, combined with interleaving, would complement the equalization and diversity measures considered here to provide additional immunity to fast fading. A demonstration of the benefits of coding in combination with equalization and diversity combining for slow-fading indoor wireless channels has been presented in [6].

System Description

The specifications of our communications system are similar, but not identical, to those of the proposed narrow-band TDMA system for North America DCR communications [1]. A block diagram of the DCR communications system is presented in Fig. 1. Specifically, a carrier transmits an overall bit rate of 48 kb/s in an allotted channel bandwidth of 30 kHz. For a $\pi/4$-shifted DQPSK modulation scheme, the symbol rate and minimum transmission bandwidth are 24 ks/s and 24 kHz, respectively. Transmit and receive filters with 25% excess bandwidth are chosen to correspond with a transmission bandwidth of 30 kHz. In particular, square-root raised-cosine (SRRC) $T/2$-spaced FIR filters with a combined Nyquist response are used.

Signaling Format

A signaling format which interleaves training sequences with data sequences within a long TDMA time slot is used (see Fig. 2). Each data frame consists of a known training sequence of length N_t symbols followed by a data sequence of length N_d symbols. Consequently, the number of symbols in each transmitted frame is:

$$\beta = N_t + N_d. \tag{1}$$

Such periodic training improves the adaptation problem by updating the CIR estimates at the beginning of each data frame. However, it incurs the expense of added system overhead, which is defined as the percentage data throughput:

$$\%T = \frac{100N_d}{N_d + N_t}\% = \frac{100N_d}{\beta}\% \tag{2}$$

Channel Model

The DCR channel is modeled in complex baseband representation with an FIR filter in the form of a $T/2$-spaced

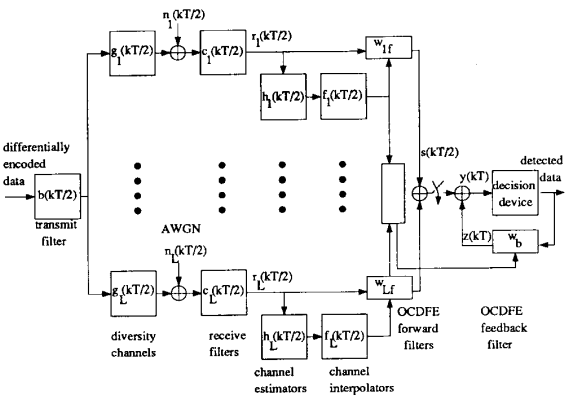

Fig. 1. Complex baseband model of a DCR communications system.

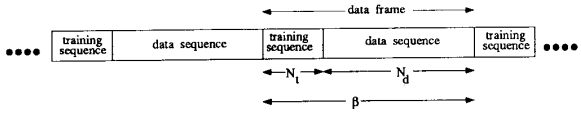

Fig. 2. Signaling format.

tapped delay line (TDL). The multipath power delay profile (MPDP) of the channel is specified with a three-path, "mountainous terrain" model with relative rms powers of 0, -5, and -15 dB [7]. The "mountainous terrain" model is considered a severly frequency-selective example [7]. In particular, for a symbol period, T, of 41.7 μs, this MPDP has an rms delay spread of 10.40 μs. Moreover, the overall CIR length, including the transmit and receiver filters, is assumed to be six symbol periods. Any remaining energy in the overall CIR which is not accounted for within the six symbol periods can be thought of as part of the CIR estimation noise. Furthermore, Rayleigh fading of each channel tap coefficient is simulated with the "sum" of sines" model using nine sinusoids with distinct Doppler frequencies ranging up to a maximum Doppler frequency, f_{dm}, of 100 Hz [8], [9]. In addition, complex AWGN with variance σ_n^2 is added to the transmitted signal at the output of each diversity channel.

Channel Estimation

In our DCR system, channel estimation is performed with a block least-squares adaptive algorithm which is optimum under the assumption that the CIR is fixed during the training period [10]. For a rapidly fading channel, this assumption is not valid and, consequently, this CIR estimation incurs an adaptation error from lagging the time variations of the channel by roughly half the observation period of the training. In fact, with a minimum length training sequence for our DCR system, it has been shown that such CIR estimation suffers from a 3 dB MSE degradation at the equalizer output upon completion of a training period [10]. This performance degradation is measured relative to the MMSE at the equalizer output for the case of a known CIR.

For our DCR system with an overall CIR length of $N_c = 6$, channel estimation is performed with an optimum BPSK

training sequence of length $N_t = 15$ [10]. The BPSK training sequence is converted into a complex, $\pi/4$-shifted DQPSK sequence by an appropriate phase transformation [11]. Consequently, given a known BPSK training sequence, the inverse autocorrelation matrix can be precomputed and stored at the receiver. Thus, during a training sequence, the CIR estimate, $\boldsymbol{h}$, which includes the transmit and receive filter responses, can be obtained from the block least-squares solution:

$$\boldsymbol{h} = \Phi_{\Delta}^{-1}\, \boldsymbol{p}_t \tag{3}$$

where Φ_{Δ} is the autocorrelation matrix of the appropriately transformed, $\pi/4$ -shifted DQPSK training sequence, and $\boldsymbol{p}_t$ is the cross-correlation vector which is computed from the received data samples during the training observation interval of $N_t - N_c + 1$ symbol periods

Channel Interpolation

During a data sequence, interpolation is performed to obtain CIR estimates which are used to compute optimum coefficients of the diversity combiner and decision-feedback equalizer (OCDFE). Without loss of generality, the number of trained CIR estimates used for each interpolation, $Q = 2p$, is assumed to be an even number so that the interpolation can be performed for the middle data frame. Consequently, each interpolated CIR estimate in the middle interpolation interval is computed from $Q/2$ past and $Q/2$ future CIR estimates obtained from training. Thus, it is evident that this CIR interpolation approach incurs an inherent processing delay. In the worst case when all Q CIR estimates from training are not known at the time of the desired interpolation, the interpolation delay, in seconds, is

$$D_t = (Q - 1)\beta T. \tag{4}$$

To satisfy Nyquist's criterion, the normalized sampling rate of the trained CIR estimates is required to be

$$\bar{f} = \frac{f_s}{2f_{dm}} = \frac{1}{2f_{dm}\beta T} \geq 1. \tag{5}$$

For the specific case of $N_t = 15$ and $Q = 4$, Fig. 3 lists representative values of the above-mentioned system parameters.

In the CIR interpolation strategy, Q consecutively estimated CIR samples obtained from periodic training, $\boldsymbol{h}(qT_s)$, are interpolated by a real-valued digital filter, $f(rT_s')$, to generate R evenly spaced, interpolated CIR samples, $\hat{\boldsymbol{h}}(rT_s')$, between the two middle, estimated CIR samples (see example in Fig. 4 which shows the relative positions of the estimated and interpolated CIR samples within a TDMA time slot). Specifically, each estimated $T/2$-spaced CIR sample, $\boldsymbol{h}(qT_s)$, has a length, N_c, of six symbol periods. Thus, each estimated CIR sample is a vector of length $2N_c = 12$ tap coefficients. Since the Rayleigh fading CIR is modeled in complex baseband, each CIR tap coefficient consists of in-phase and quadrature components which are characterized as independent, zero-mean, Gaussian random processes. Consequently, each CIR interpolation is performed for 24 randomly fading, real-valued coefficients. Furthermore, the interpolation factor, R, is defined as [12]:

interpolation interval length ("beta")	120	100	80	60	40
normalized sampling rate ("fs/(2*fdm)")	1.0	1.2	1.5	2.0	3.0
percentage throughput ("%T")	87.5	85.0	81.3	75.0	62.5
interpolation delay ("Dt") [milliseconds]	15.0	12.5	10.0	7.5	5.0

Fig. 3. Representative values of system parameters; for $Nt = 15$, $Q = 4$, $1/T = 24$Ks/s, $f_{dm} = 100$ Hz.

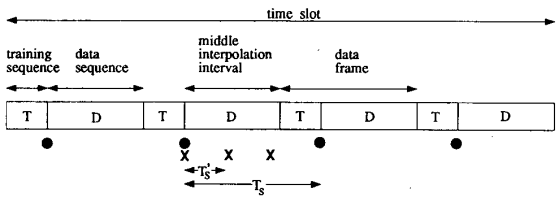

Fig. 4. CIR interpolation within a TDMA time slot. ●-estimated CIR sample at the end of a training sequence, $Q = 2p = 4$. X-interpolated CIR sample in the middle, data frame, $R = T_s/T_s' = Bl\mu = 3$.

$$R = \frac{T_s}{T_s'} = \frac{\beta T}{\mu T} = \frac{\beta}{\mu} = \frac{N_t + N_d}{\mu} \tag{6}$$

where

- T_s the sampling period of the estimated CIR samples
- T_s' the sampling period of the interpolated CIR samples
- T the symbol period
- β the number of symbol periods between estimated CIR samples
- μ the number of symbol periods between interpolated CIR samples
- N_t the number of symbols in a training sequence
- N_d the number of symbols in a data sequence.

The interpolated CIR sequence $\hat{\boldsymbol{h}}(rT_s')$, is computed as the convolution of the oversampled input sequence of Q CIR samples, $\bar{\boldsymbol{h}}(rT_s')$, with the unit sample response of the interpolator, $f(rT_s')$ [12]:

$$\hat{\boldsymbol{h}}(rT_s') = \bar{\boldsymbol{h}}(rT_s') * f(rT_s') = \boldsymbol{h}\left(\frac{rT_s'}{R}\right) * f(rT_s'), \qquad r = 0, 1, \cdots, R-1 \tag{7}$$

where the interpolated output sequence, $\hat{\boldsymbol{h}}(rT_s')$, is evaluated over one interpolation interval (i.e., a data sequence) to generate R interpolated CIR samples.

For the CIR interpolation in our DCR system, a practical digital filter, $f(rT_s')$, is employed with a truncated discrete-time window, $\Pi(rT_s'; \eta)$, which corresponds to an approximately raised-cosine frequency response of the overall interpolator (i.e., a truncated Nyquist pulse):

$$f(rT_s') = \tilde{f}(rT_s')\Pi(rT_s'; \eta), \qquad r = 0, \pm 1, \pm 2, \ldots \tag{8}$$

where the unit sample response of the ideal low-pass filter is

$$\tilde{f}(rT_s') = \frac{\sin\left(\frac{\pi r T_s'}{R}\right)}{\frac{\pi r T_s'}{R}}, \qquad r = 0, \pm 1, \pm 2, \ldots \quad (9)$$

and the discrete-time window response is

$$\Pi(rT_s';\eta) = \begin{cases} \dfrac{\cos\left(\frac{\eta\pi r T_s'}{R}\right)}{1-\left(\frac{2\eta r T_s'}{R}\right)^2}, & -\left(\dfrac{N_p-1}{2}\right) \le r \le \left(\dfrac{N_p-1}{2}\right) \\ 0, & \text{otherwise} \end{cases} \quad (10)$$

where N_p is the length of the unit sample response of the interpolator and $0 \le \eta \le 1$ is the rolloff factor of the interpolation window.

OCDFE Computation

In our DCR system, the OCDFE parameters are adaptively computed using interpolated CIR estimates, $\hat{h}_l(kT)$, from each of the L diversity channels, to yield optimum performance in the MMSE sense. The OCDFE has a fractionally spaced forward filter, w_l, in each of its L diversity branches and a synchronous feedback filter, w_b, in a common feedback loop emanating from the output of the decision device[2] (see Fig. 1). Each forward filter is implemented as a $T/2$-spaced TDL with N_f tap coefficients while the feedback filter is implemented as a T-spaced TDL with N_b tap coefficients. At the lth diversity branch, the received signal is:

$$r_l(t) = \sum_k \Delta_a(kT)\hat{h}_l(t - kT) + n_l(t) \quad (11)$$

where $\Delta_a(kT)$ is the $\pi/4$-shifted DQPSK transmitted symbol at time kT and the $2/T$-sampled, received-filtered, additive Gaussian noise, $n_l(t - kT/2)$, has a variance of σ_n^2 and an autocorrelation function, $\Phi_n((k-l)T/2)$, with a 25% excess bandwidth raised-cosine response.

By minimizing the MSE at the output of the OCDFE, it can be shown that, for a given set of interpolated CIR's and noise statistics in the L diversity channels, the optimum OCDFE coefficients are computed as

$$w_{\text{opt}} = \Phi^{-1}p \quad (12)$$

where the $(LN_f + N_b) \times (LN_f + N_b)$ Hermitian, positive-semidefinite autocorrelation matrix, Φ, can be partitioned into submatrices. Specifically, the (i, j)th element of the submatrix, $\Phi_{l,q}$, for diversity signal correlation, is

$$\Phi_{l,q}(i,j) = \sum_k \hat{h}_l\left(kT - i\frac{T}{2}\right)\hat{h}_q^*\left(kT - j\frac{T}{2}\right) + \sigma_n^2\Phi_n\left((i-j)\frac{T}{2}\right),$$

$$= \Phi_{q,l}^*(j,i), \qquad i,j = 0,1,\cdots,N_f-1 \quad l,q = 0,1,\cdots,L-1 \quad (13)$$

and the (i, j)th element of the submatrix, $\Phi_{i,b}$, for diversity signal and feedback data correlation, is a sample coefficient of the lth interpolated CIR.[3]

$$\Phi_{l,b}(i,j) = \hat{h}_l\left((D+1)T - i\frac{T}{2} + jT\right), \quad i = 0,1,\cdots,N_f-1$$

$$= \Phi_{b,l}^*(j,i) \qquad j = 0,1,\cdots,N_b-1 \quad l = 0,1,\cdots,L-1 \quad (14)$$

and $\Phi_{b,b} = I$ is an $N_b \times N_b$ identity matrix.

For the case of antenna diversity with independently fading received branch signals, the ensemble averages (with respect to the fading CIR) of the off-diagonal submatrices are zero-valued:

$$E[\Phi_{l,q}(i,j)] = 0, \qquad l \ne q \quad i,j = 0,1,\cdots,N_f-1. \quad (15)$$

Furthermore, for the $LN_f + N_b) \times 1$ partitioned cross-correlation vector, the ith element of its lth subector is a $T/2$-spaced sample coefficient of the lth interpolated CIR:

$$p_l(i) = \hat{h}_l\left(DT - i\frac{T}{2}\right), \qquad i = 0,1,\cdots,N_f-1 \quad l = 0,1,\cdots,L-1 \quad (16)$$

while the last cross-correlation subvector is a zero-vector, $p_b = 0$.

Simulation Results

Fixed Interpolator Simulation

In order to determine a suitable CIR interpolator for our DCR system, the interpolation performance of relatively simple digital filters which employ approximately raised-cosine and generalized Hamming windows was initially investigated. From interpolation simulations of Q = four ideal estimates of a single Rayleigh fading tap coefficient exhibiting a worst-case Doppler frequency of f_{dm} = 100 Hz, it was found that the raised-cosine interpolator (see (10)) performed better at all sampling rates [11]. Moreover, despite its non-adaptive nature, such an interpolator possesses an optimum rolloff factor which is a function of the sampling rate. Typical performance curves for the raised-cosine interpolator, operating under ideal conditions of zero estimation noise, are shown in Fig. 6, where the time-averaged mean squared error, $\overline{mse}$, is averaged over the R interpolated samples within an interpolation interval for an ensemble of N = 1000 trials:

$$\overline{mse} = \frac{1}{RN}\sum_{r=0}^{R-1}\sum_{n=0}^{N-1}\left|\hat{h}_n(kT + rT_s') - g_n(kT + rT_s')\right|^2 \quad (17)$$

[2] For the sake of notational simplicity, the time dependence of the OCDFE weight vectors is implicit.

[3] DT is the processing delay of the OCDFE.

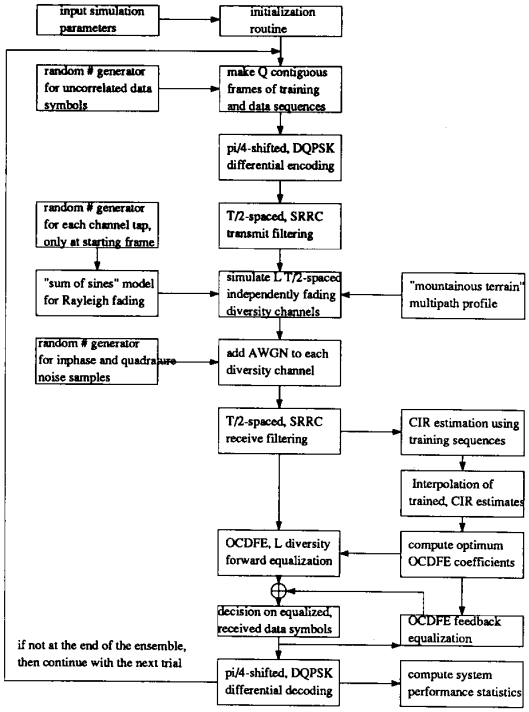

Fig. 5. DCR system simulation flowchart.

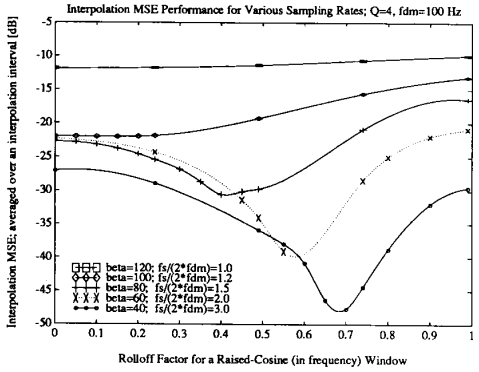

Fig. 6. MSE performance for a raised cosine interpolator.

where $\hat{h}_n$ is the interpolated CIR tap coefficient for the nth, simulation trail and g_n is the actual CIR tap coefficient for the nth simulation trial.

From Fig. 6, it is evident that for a given interpolator, the interpolation MSE performance generally improves with increasing sampling rates. This is a reasonable result since if the frequency of training is increased, then the tracking of a time varying signal should improve. Specifically, the poor performance near $\bar{f} = 1.0$ can be explained by considering the frequency responses of the time-varying signal and interpolator. Near the minimum sampling rate, the Doppler spectral images of the time-varying tap coefficient are very close together. Thus, in order to remove all the spectral images so as to reconstruct the tap coefficient response faithfully at the interpolated samples, the interpolator must have a frequency response which resembles that of an ideal lowpass filter. On the other hand, the filtering problem becomes less severe as the sampling rate is increased. In this case, the interpolation performance improves because, as the Doppler spectral images of the fading tap coefficient separate in frequency, the distortion caused by aliasing is reduced.

For the raised-cosine interpolator, it is evident from Fig. 6 that as the sampling rate increases, the optimum value of the rolloff factor also increases. The reason for this is that at low sampling rates, the interpolation MSE is dominated by aliasing while as the sampling rate increases, the interpolation MSE becomes relatively less affected by aliasing and progressively more limited by pass-band distortion. Specifically, the optimum interpolator rolloff at a given sampling rate occurs when the impairments of aliasing and passband distortion are jointly minimized. The simulation results also show that as the sampling rate increases, the MSE gain by selecting the optimum rolloff factor for the interpolator also increases. For example, at the Nyquist rate corresponding to $\bar{f} = 1.0$, the difference in MSE performance between interpolators with the optimum rolloff of $\eta_{\text{opt}} = 0.0$ and the worst-case rolloff of $\eta = 1.0$ is less than 2 dB. However, at the normalized sampling rate of $\bar{f} = 3.0$, the difference in MSE performance between interpolators with the optimum rolloff of $\eta_{\text{opt}} = 0.7$ and the worst-case rolloff of $\eta = 0.0$ is over 20 dB. This highlights the important filter design issue of selecting the proper window parameter for a given interpolator operating at a specific sampling rate.

However, for the realistic case of significant estimation noise, it was found that the interpolation performance gains obtained from the optimum choices of the filter rolloff are negligible. This dominant effect of the estimation noise on interpolation performance is illustrated in Fig. 7, where the signal-to-estimation-noise-ratio (SER) for one fading tap coefficient is defined as:

$$\text{SER} = 10 \log_{10}\left(\frac{\sigma_g^2}{\sigma_e^2}\right) \text{dB} \tag{18}$$

with $\sigma_g^2 = 1$ being the normalized variance of each CIR tap coefficient and σ_e^2 being the variance of the estimation noise for each CIR tap coefficient. In the simple case of a one-tap fading channel with estimation noise but no AWGN, the SER is just the SNR. For a channel with N_c tap coefficients and assuming a sufficiently long training sequence, the SER is roughly N_c times that of the SER for one tap coefficient.

As can be seen in Fig. 7, the effect of estimation noise on interpolation performance can be quite significant. In general, estimation noise dominates the tracking problem at low SER, while the interpolation MSE performance is much better at higher values of SER. This is especially true for interpolators operating at high sampling rates. For instance, a 50% rolloff raised-cosine interpolator sampling at twice the Nyquist rate, i.e., $\bar{f} = 2.0$, can lose over 20 dB in MSE performance by going from an SER of 30 dB to 3 dB (see Fig. 7). This clearly illustrates the strong influence of estimation noise on the interpolator performance.

Moreover, estimation noise can indeed nullify the significant interpolation gains obtained from using optimum rolloff

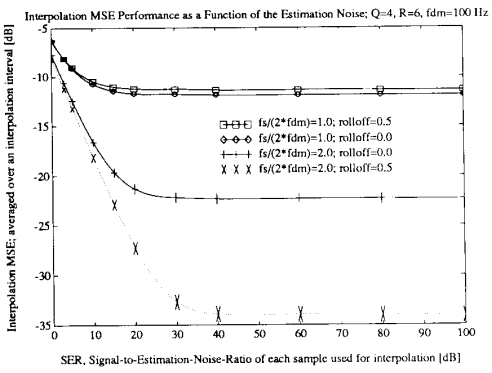

Fig. 7. Interpolation performance as a function of the estimation noise.

values and a large interpolation factor. Since it has been found that interpolation error can be minimal when estimation noise is not present (see Fig. 6), the degree of SER can determine whether or not a DCR system suffers an irreducible BER at high SNR (assuming ISI is not a limiting factor). In order to achieve interpolation performance at a negligible[4] MSE of less than -30 dB, an SER of over 30 dB is required.

In addition, it was found that at high SER levels, the interpolation *mse* performance improves significantly for each of the following cases [11]:

1) at a lower maximum Doppler frequency, f_{dm},
2) at a high sampling rate, f_s,
3) for a larger number of samples used per interpolation, Q, and
4) for a larger interpolation factor, R.

Specifically, the interpolation factor, R, can significantly affect the tracking performance since, for a given value of β, the lag error of the interpolator is inversely proportional to R. For a typical example with $\beta = 60$ and $R = 12$, the spacing between interpolated samples is $\mu = \beta/R = 5$. Moreover, for a maximum Doppler frequency of 100 Hz, the CIR can vary up to 13% of its maximum amplitude in an interval of $\mu = 5$ symbol periods. Thus, for a given throughput constraint (i.e., fixed β and N_t), the choice of R can determine the degree of lag error in the interpolation process. Of course, choosing a large R can reduce this lag error, but at the expense of added computational overhead at the receiver. Nevertheless, it was found from simulation that, at low SER levels, the estimation noise tends to nullify the above interpolation performance gains. In an actual DCR system, the estimation noise floor is mainly caused by a lag error in the training process of the CIR estimation. Thus, a decrease in the fade rate should reduce the CIR estimation noise.

System Simulation

The performance of our DCR system is investigated via computer simulation (see Fig. 5). In particular, the DCR system is modeled with equivalent complex baseband signals and simulated using a Monte Carlo approach with between 2000 and 10 000 independent trials generated for each ensemble. Each trial entails the transmission of Q contiguous data frames, each of which consists of an initial training sequence followed by an uncorrelated data sequence, $\boldsymbol{a}(kT)$. The symbols in this set of contiguous data frames are $\pi/4$-shifted DQPSK-encoded and transmit-filtered using a $T/2$-spaced, 55 taps FIR filter with an SRRC impulse response. Specifically, the transmitted symbols, $\boldsymbol{\Delta}_a(kT)$, are $2/T$-sampled such that each data sample is followed by a zero-valued, $T/2$-spaced sample. Thus, pulse modulation (e.g., DQPSK) is simulated with the transmitted pulse modulated by the data symbol impulse.

Each data frame is transmitted over L independently fading, $T/2$-spaced diversity channels, $\boldsymbol{g}_l(kT)$, each with tap coefficients which exhibit independent Rayleigh fading with a given Doppler frequency, simulated as in [8], [9]. The sets of channels are independent from trial to trial. The $T/2$-spaced symbols at the output of each diversity channel are corrupted with $T/2$-spaced AWGN samples, $n_l(kT)$, and receive-filtered using a $T/2$-spaced, 64 tap, FIR filter with an SRRC impulse response. In addition, the received signal, $\boldsymbol{r}_l(kT - m(T/2))$, at each diversity branch is represented as two interleaved, T-spaced sequences which are offset by $T/2$-phase.

At each diversity channel and for each of Q data frames in a trial, the two $T/2$-offset received training sequences are used to estimate Q consecutive CIR's, $\boldsymbol{h}_l(qT_s)$, which are spaced a data frame, i.e., βT symbols, apart. Subsequent to this training, the trained CIR estimates are filtered by a real-valued, windowed $\sin x/x$ interpolator, $f(rT_s')$, to generate R interpolated CIR estimates, $\hat{\boldsymbol{h}}(rT_s')$, which are spaced μT symbols apart within the middle data frame of the trial. Given the interpolated CIR estimates for each of the L diversity channels, the OCDFE coefficients, $\boldsymbol{w}_{\text{opt}}$, are computed every μT symbols (i.e., at every interpolated CIR sample).

Each received data symbol in the middle data frame is processed by the OCDFE to yield an optimally combined and equalized signal, $y(kT)$, which can then be detected by the decision device. Following this, the decision output, $\hat{\Delta}_a((k - D)T)$, is $\pi/4$-shifted DQPSK-decoded to yield the QPSK decision symbol, $\hat{a}((k - D)T)$.

The simulation trial is complete when all N_d data symbols, $a(kT)$, of the middle data frame are processed. Subsequently, the simulation program proceeds onto the next trial in the ensemble. Upon completion of all the trials, the simulation finishes with the computation of the DCR system performance measures, viz., the average MSE, average BER and outage probability. Even though the fast fading DCR channel can exhibit burst errors, the average probability of bit error (BER) was found to yield results consistent with those of the outage probability of a user frame [11]. Thus, in this paper, results are presented for only the average BER. Moreover, for DQPSK signaling, the average BER is assumed to be half the average probability of symbol error.

In this section, simulation results of our DCR system are

[4] An interpolation MSE of less than -30 dB is negligible for an SNR of about 20 dB. The interpolation MSE is negligible in the sense that it would not be the cause of an irreducible BER at this operating range.

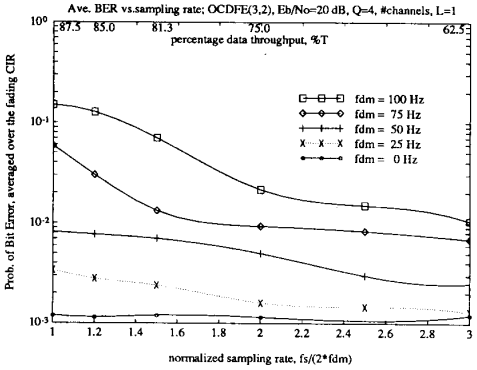

Fig. 8. Average BER as a function of interpolation sampling rate and Doppler fading.

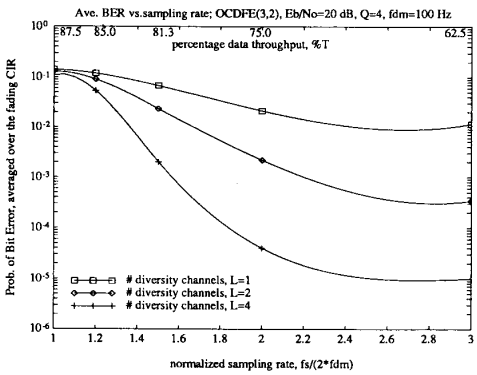

Fig. 9. Average BER as a function of interpolation sampling rate and diversity.

presented for the case of CIR interpolation with a zero rolloff raised-cosine interpolator. Unless otherwise stated, the OCDFE consists of $N_f = 3$ taps in the forward filter at each diversity branch and $N_b = 2$ taps in the feedback filter. This configuration is denoted as OCDFE(3,2). In addition, the following nominal parameter values are used: $N_c = 6$, $N_t = 15$, $Q = 4$, $\mu = 5$ and $f_{dm} = 100$ Hz.

The average BER performance as a function of the normalized sampling rate, $\bar{f}$, for different values of the maximum Doppler frequency, f_{dm}, is illustrated in Fig. 8 for the case of $E_b/N_0 = 20$ dB and $L = 1$. It is evident from this figure that the average BER is monotonically decreasing for increasing values of $\bar{f}$. Furthermore, this average BER improvement is greater at larger values of f_{dm}. In particular, for a worst-case maximum Doppler frequency of $f_{dm} = 100$ Hz, the average BER decreases from 1.5×10^{-1} to 10^{-2} when $\bar{f}$ goes from 1.0 to 3.0. This improvement is due to more frequent training and improved CIR tracking with the removal of aliasing distortion in the interpolation filter.

In addition, it is also evident from Fig. 8 that the system performance is less influenced by the sampling rate, $\bar{f}$, at progressively lower values of the maximum Doppler frequency, f_{dm}. In fact, at $f_{dm} = 0$ Hz (i.e., nonfading CIR), the average BER is independent of $\bar{f}$, since tracking is not an issue for a time-invariant channel. However, for a fading channel, the value of f_{dm} can strongly affect the system performance. For instance, at values of $\bar{f} \approx 1.0$ near the Nyquist sampling rate, where aliasing distortion is significant in the CIR interpolation process, a reduction in the f_{dm} from a worst-case value of 100 to 50 Hz reduces the average BER by over an order of magnitude from about 10^{-1} to less than 10^{-2}. At a more practical value of $\bar{f} = 2.0$ where the aliasing distortion due to the CIR interpolator is negligible and where the higher frequency of training reduces the effect of fading, a reduction in the f_{dm} from a worst-case value of 100 to 50 Hz, nonetheless, reduces the average BER by about five times from 2×10^{-2} to 5×10^{-3}. Thus, vehicular speed can significantly affect the fading problem in a DCR system. In other words, CIR estimation and tracking are crucial to reliable DCR communications.

The system performance gain with increasing $\bar{f}$ incurs an overhead of reduced system throughput, $\%T$. This associated overhead is displayed on the upper horizontal axis in Figs. 8 and 9. Furthermore, the choice of $\bar{f}$ also affects the interpolation processing delay, D_t. Specifically, at $\bar{f} = 1.0$, the percentage data throughput, $\%T$, is 87.5% and the worst-case interpolation delay, D_t, is 15 ms while at $\bar{f} = 3.0$, $\%T$ is only 62.5% and D_t is 5 ms. Thus, depending on the throughput and processing delay constraints for a particular application, one can select the appropriate sampling rate which will adequately trade-off between system performance and throughput/delay requirements. From the results presented, a value of $\bar{f} = 2.0$ (i.e., twice the Nyquist sampling rate), with an associated $\%T = 75\%$ and $D_t = 7.5$ ms, is a reasonable design choice for our DCR system. In addition, the use of diversity channels (i.e., $L > 1$) also incurs added hardware complexity in implementing diversity antennas at the mobile receiver.

Average BER performance curves as functions of the normalized sampling rate, $\bar{f}$, and the number of diversity channels, L, are shown in Fig. 9 for the case of $E_b/N_0 = 20$ dB and $f_{dm} = 100$ Hz. It is evident from this figure that the system performance improves with increasing $\bar{f}$ and L. However, at the Nyquist sampling rate (i.e., $\bar{f} = 1.0$) for all diversity cases, the system performance is unacceptable with an average BER of over 10^{-1}. This mediocre performance is caused by insufficiently frequent training and by the severe aliasing distortion due to the interpolation filter which leads to poor tracking of the fast fading channel at each diversity branch. Thus, adding more independently fading channels only improves the tracking performance marginally. On the other hand, for $L = 1$ and $\bar{f} \geq 2.0$, the average BER is on the order of 10^{-2} and is thus acceptable for voice communications. However, at high sampling rates, the DCR system performance gains do tend to flatten out.

In addition, the use of diversity can greatly improve the system performance. As shown in Fig. 9, at a reasonable value of $\bar{f} = 2.0$, the use of $L = 2$ diversity channels can reduce the average BER by an order of magnitude to 2×10^{-3}. Furthermore, the use of $L = 4$ diversity channels at the same value of $\bar{f}$ can achieve an average BER of 4×10^{-5}. Thus, at this operating range, reliable data communications is possible with a relatively small increase in receiver overhead to implement diversity antennas.

The remaining results in this section illustrate the system performance as a function of the average channel SNR, E_b/N_0, for the case of a normalized sampling rate of $\bar{f} = 2.0$ and at varying degrees of channel fading, diversity and equalization. In all cases, the system performance was found to improve with increasing E_b/N_0. However, an irreducible BER was also found to occur at high values of $E_b/N_0 \geq 20$ dB. This performance floor is likely due to limitations in the ability of the receiver to estimate and track the rapid time variations in the fading channel.

The average BER performance as a function of E_b/N_0 for different values of the maximum Doppler frequency, f_{dm}, and diversity order, L, is illustrated in Fig. 10. This figure consists essentially of two sets ($L = 1, 2$) of three curves ($f_{dm} = 10, 50, 100$ Hz). For a given diversity order, L, there is little difference in the system performance for all values of f_{dm} at low values of E_b/N_0. This is primarily because, at this operating range, the high channel noise is the determining factor in the poor system performance, regardless of the CIR estimation and tracking. As the value of E_b/N_0 increases, the degree of fading has a dramatic effect on the system performance. Specifically, for a given E_b/N_0 and L, the average BER decreases sharply for decreasing values of f_{dm}. Furthermore, for $f_{dm} \geq 50$ Hz, an irreducible BER is evident for $E_b/N_0 \geq 20$ dB. However, an irreducible BER is still evident at higher values of E_b/N_0 for slower fading channels, e.g., $E_b/N_0 \geq 30$ dB when $f_{dm} = 10$ Hz.

The above result implies that the irreducible BER may be caused by the CIR estimation and tracking. At higher values of f_{dm}, the task of following a rapidly fading CIR can be much more difficult and, thus, leads to a higher estimation and tracking (i.e., interpolation) noise. This increase in the lag error causes the onset of the irreducible BER to occur at a lower value of E_b/N_0 where the estimation and tracking noise overtakes the thermal noise as being the limiting factor in the system performance. As shown in Fig. 10, the irreducible BER of 2×10^{-3} for the case of $f_{dm} = 100$ Hz and $L = 2$ is actually lower than that of 5×10^{-3} for the case of $f_{dm} = 50$ Hz and $L = 1$. Thus, despite the strong influence of f_{dm} on the irreducible BER, the use of channel diversity can effectively overcome the fast fading in a DCR channel. Even though it does not remove the irreducible BER, the use of diversity does significantly reduce the level of the irreducible BER.

The average BER performance as a function of E_b/N_0 for varying numbers of diversity channels, L, is also shown in Fig. 11, along with lower bound performance curves for coherent QPSK signaling in a slowly fading, nondispersive AWGN channel [13]. With our use of differential encoding in a relatively bursty channel, this lower bound should actually increase by up to a factor of two in the average BER. The comparison between the lower bound curves and the simulation curves clearly show the drastic effect of the irreducible BER on system performance at high values of E_b/N_0. In particular, for a given L at low E_b/N_0 where the CIR estimation and tracking noise is less significant relative to the thermal noise, the difference between the simulated performance and the lower performance bound is relatively small, e.g., about an order of magnitude at $E_b/N_0 = 5$ dB for $L = 2$. However, at high values of E_b/N_0 where the CIR estimation and tracking noise is dominant over the thermal noise, the difference between the simulated performance and the lower performance bound is strikingly large. As an example, for $L = 2$ at an $E_b/N_0 = 30$ dB, the difference in average BER performance is over four orders of magnitude. Furthermore, since the theoretical performance improvement with E_b/N_0 grows with increasing values of L, the difference in performance between the irreducible BER performance of the simulated results and the theoretical lower bound also grows with increasing values of L. These comparisons further illustrate the severe impact on system performance due to the adaptation lag error.

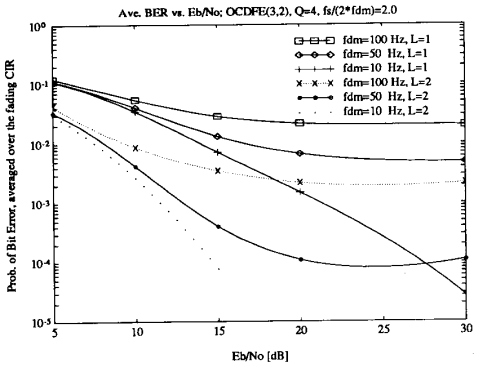

Fig. 10. Average BER as a function of channel SNR, diversity, and Doppler fading.

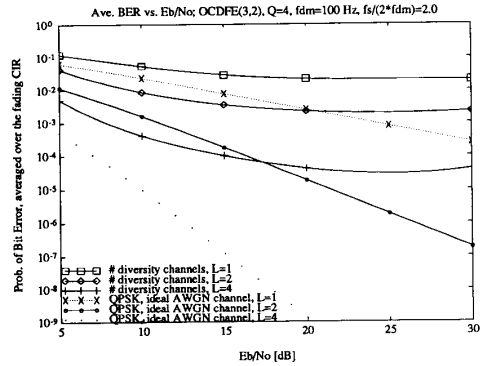

Fig. 11. Average BER as a function of channel SNR and diversity.

The effects of ISI and channel fading on the system performance are illustrated in Fig. 12. Specifically, the average BER performance as a function of E_b/N_0 of receivers with and without decision-feedback equalization is shown for different diversity orders, L. When no equalization and no diversity is implemented, i.e., OCDFE(1,0) and $L = 1$, the system performance is severely degraded with an average BER of greater than 10^{-1} at most values of E_b/N_0. Thus, the effects of time dispersion and Doppler fading in a DCR channel need to be reduced in order to achieve acceptable system performance. Moreover, despite the significant bene-

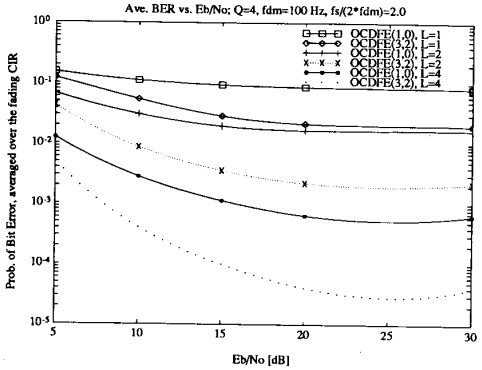

Fig. 12. Average BER as a function of channel SNR, with and without equalization.

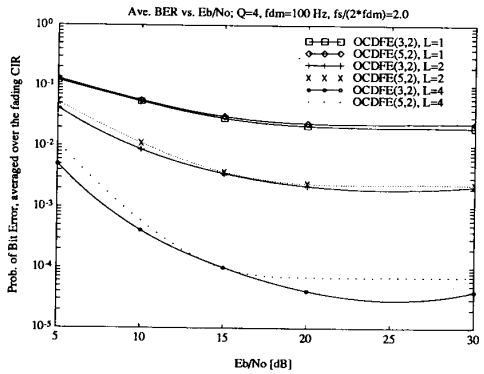

Fig. 13. Average BER as a function of channel SNR and OCDFE configuration.

fit of explicit diversity combining, a two-channel OCDFE without equalization has only marginally superior performance over a single-channel OCDFE with equalization. This comparison is especially true at high values of E_b/N_0 where the thermal noise is negligible. However, at low values of E_b/N_0 where there is a significant presence of thermal noise, the performance gain by using an equalizer is less since the equalizer incurs more self-noise in its tap coefficients. Nevertheless, these results indicate that the ISI caused by the multipath channel, in conjunction with the transmit and receive filters, is quite significant if the overall channel is not equalized. In fact, the performance improvement by using equalization can be more than an order of magnitude in average BER when using four diversity channels and operating at $E_b/N_0 \geq 15$ dB.

From the above results, it is evident that the use of both equalization and diversity combining is important to achieving good system performance. However, there is the possibility that an OCDFE(3,2) receiver might not remove all of the existing ISI. If this were the case, then the residual ISI could account for the irreducible BER at $E_b/N_0 \geq 20$ dB. The comparison of receivers with varying degrees of equalization and diversity is shown in Fig. 13. These results indicate that the OCDFE(3,2) receiver removes most of the ISI, since a longer equalizer with the same diversity order, e.g., OCDFE(5,2), does not improve the system performance at high values of $E_b/N_0 \geq 20$ dB. In fact, a longer equalizer performs worse at most values of E_b/N_0. This poor performance occurs because a longer equalizer, with more tap coefficients, experiences more self-noise in the computation of its tap coefficients. This argument applies for an equalizer with more feed-forward or feedback taps. Thus, our results indicate that the OCDFE(3,2) receiver is optimum in terms of correcting for ISI.

The performance of a system employing transmit and receive filters with higher rolloff factors (e.g., 50%) was also investigated. The simulation results indicate that the use of less stringent filtering only improves the system performance marginally. This performance improvement is achieved because higher rolloff filters have lower sidelobes in their impulse responses which lead to a less severe ISI problem. However, this performance improvement incurs a penalty of increased susceptibility to ACI since the filter bandwidth is larger. In addition, a system employing interpolation filters with their optimum rolloff values was studied. A negligible difference in performance was found between using zero rolloff and optimum rolloff interpolators. Furthermore, due to the dominance of the CIR estimation noise, very little difference in system performance was observed when the spacing, μ, between interpolated samples or the number of CIR estimates used for each interpolation, Q, were varied.

In summary, our results indicate that the system performance is limited by the CIR estimation and not by the CIR interpolation or residual ISI due to suboptimum equalization. Specifically, because the fast fading channel is varying during a training sequence, the CIR estimate obtained at the end of a training sequence lags the actual CIR by about half the observation period of the training. For a training sequence of $N_t = 15$, the observation period is $N_t - N_c + 1 = 10$ [10]. Thus, for a worst-case maximum Doppler frequency of 100 Hz, the CIR can change by up to about 13% in amplitude during training [11]. Moreover, because of the limited length of the training sequence, the CIR estimation can have a significant variance. The result of all this is that the CIR estimation noise is a likely source of the irreducible error rate at values of $E_b/N_0 \geq 20$ dB.

Conclusion

We conclude that reliable voice communications for a low bit-rate, narrow-band DCR system can be achieved with our proposed receiver and block adaptation scheme, while incurring relatively little system overhead. We have shown that a relatively simple fractionally spaced decision-feedback equalizer can minimize the effect of intersymbol interference, while diversity combining can significantly improve system performance under rapidly fading conditions. In addition, we have proposed and demonstrated a novel block-adaptive method which employs CIR estimation and interpolation to identify the time-varying CIR and periodically computes the receiver parameters of a DCR system. We have also found that the adaptation process is limited mainly by the CIR estimation noise due to imperfect training, which is manifested in the form of an irreducible bit error rate at high signal-to-noise ratios. However, we have shown that this

system performance limitation is less severe at lower channel fade rates and can be alleviated through the use of channel diversity.

ACKNOWLEDGMENT

The authors thank Gordon Davidson and Dr. Stewart Crozier for their help with the computer simulations, and Brent Petersen for his help in preparing the final manuscript.

REFERENCES

[1] Electronic Industries Association, *Cellular System: Dual-Mode Subscriber Equipment – Network Equipment Compatibility Specifications,* EIA project 2215, IS-54, Dec., 1989.

[2] P. Monsen, "Feedback equalization for fading dispersive channels," *IEEE Trans. Inform. Theory,* vol. IT-17, pp. 56–64, Jan. 1971.

[3] E. Eleftheriou and D. D. Falconer, "Tracking properties and steady state performance of RLS adaptive filter algorithms," *IEEE Trans. Acoust., Speech, Signal Processing,* vol. ASSP-34, pp. 1097–1110, Oct. 1986.

[4] S. McLaughlin, B. Mulgrew, and C. Cowan, "Performance comparison of least squares and least mean squares algorithms as HF channel estimators," in *Proc. ICASSP 87,* 1987, pp. 2105–2108.

[5] G. W. Davidson, D. D. Falconer, and A. U. H. Sheikh, "An investigation of block-adaptive decision feedback equalization for frequency selective fading channels," *Can. J. Elect. Comput. Eng.,* vol. 13, no. 3–4, pp. 106–111, Mar. 1988.

[6] C. L. Despins, D. D. Falconer, and S. A. Mahmoud, "Coding and optimum-baseband combining for wideband TDMA indoor wireless channels," in *Proc. Globecom 90,* Dec., 1990, pp. 1832–1837.

[7] R. W. Lorenz, J. deWeck, and P. Merki, "Power delay profiles measured in mountainous terrain," in *Proc. VTC 88,* 1988, pp. 105–112.

[8] W. C. Jakes, Ed., *Microwave Mobile Communications.* New York: Wiley, 1974.

[9] E. F. Casas and C. Leung, "A simple digital fading simulator for mobile radio," in *Proc. Veh. Technol. Conf. 88,* Sept. 1988, pp. 212–217.

[10] S. N. Crozier, "Short-block, data detection techniques employing channel estimation for fading, time-dispersive channels," Ph.D. dissertation, Dept. Syst. and Comput. Eng., Carleton Univ., Ottawa, ON, Canada, Rep. SCE-90-11, May 1990.

[11] N. W. K. Lo, "adaptive equalization and diversity combining for a mobile radio channel," Master's thesis, Dept. Syst. and Comput. Eng., Carleton Univ., Ottawa, ON, Canada, Rep. SCE-90-09, May 1990.

[12] R. W. Schafer and L. R. Rabiner, "A digital signal processing approach to interpolation," *Proc. IEEE,* vol. 61, pp. 692–702, Jun. 1973.

[13] J. G. Proakis, *Digital Communications.* New York : McGraw-Hill, 1983.

Norm W. K. Lo (S'89) was born in Hong Kong on December 17, 1962. He received the B.A.Sc. degree in engineering physics from the University of British Columbia, Vancouver, BC, Canada, in 1986, and the M.Eng. degree in electrical engineering from Carleton University, Ottawa, ON, Canada in 1990.

Since 1986 he has been affiliated with Bell-Northern Research, Ottawa, ON, Canada, first as a member of the Scientific Staff working in the area of CAD simulation and verification, and then from 1989 to the present, as a BNR Postgraduate Award student at Carleton University, where he is currently working toward the Ph.D. degree in electrical engineering. During the 1990–1991 academic year, he was a postgraduate exchange student at Edinburgh University, Edinburgh, Scotland. His current research interests are in digital communications and signal processing.

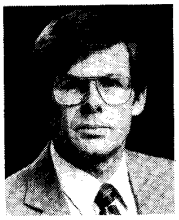

David D. Falconer (M'68–SM'83–F'86) was born in Moose Jaw, Saskatchewan, Canada on August 15, 1940. He received the B.A.Sc. degree in engineering physics from the University of Toronto, Toronto, ON, Canada, in 1962 and the S.M. and Ph.D. degrees in electrical engineering from the Massachusetts Institute of Technology, Cambridge, in 1963 and 1967, respectively.

After a year as a postdoctoral fellow at the Royal Institute of Technology, Stockholm, Sweden, he was with Bell Laboratories, Holmdel, NJ, from 1967 to 1980, as a member of the technical staff and later as group supervisor. During 1976–1977 he was a visiting professor at Linköping University, Linköping, Sweden. Since 1980 he has been at Carleton University, Ottawa, Canada, where he is a Professor in the Department of Systems and Computer Engineering. His interests are in digital communications, signal processing, and communication theory.

Dr. Falconer was Editor for Digital Communications for the IEEE TRANSACTIONS ON COMMUNICATIONS from 1981 to 1987 and was co-Guest editor the September 1984 issue of the IEEE JOURNAL OF SELECTED AREAS IN COMMUNICATION on Voiceband Telephone Transmission. He is a member of the Association of Professional Engineers of Ontario. He was awarded the Communications Society Prize Paper Award in Communications Circuits and Techniques in 1983 and in 1986.

Asrar U. H. Sheikh (M'71–M'83–SM'86) graduated from the University of Engineering and Technology, Lahore, Pakistan, and received the M.Sc. and Ph.D. degrees from the University of Birmingham, England, in 1966 and 1969, respectively.

He held Lectureships at Universities in Pakistan, Iran, and Libya between 1969 and 1975 before returning to Birmingham as a Research Fellow. He joined Carleton University, Ottawa, ON, Canada as an Associate Professor. At present he is a Professor and the Associate Chairman of Graduate Studies in the Department of Systems and Computer Engineering. He has published extensively in the areas of impulsive noise and mobile communications. His current interests are in signal processing in communications, mobile communications, and spread spectrum. He has been a consultant to several private and government agencies.

Dr. Sheikh is co-recipient of the Paul Adorian Premium from the IERE for his work on impulsive noise characterization. He is a Professional Engineer licensed in the Province of Ontario.